Expanded View Figures

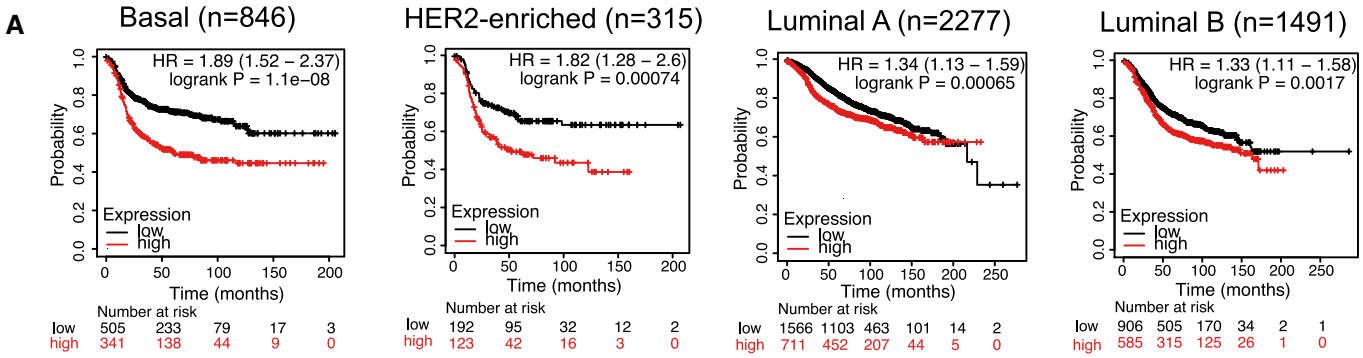

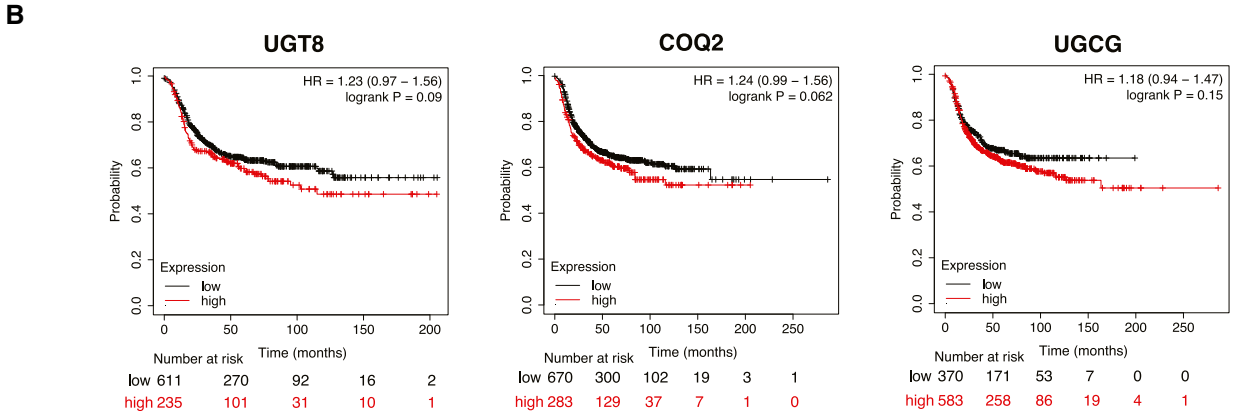

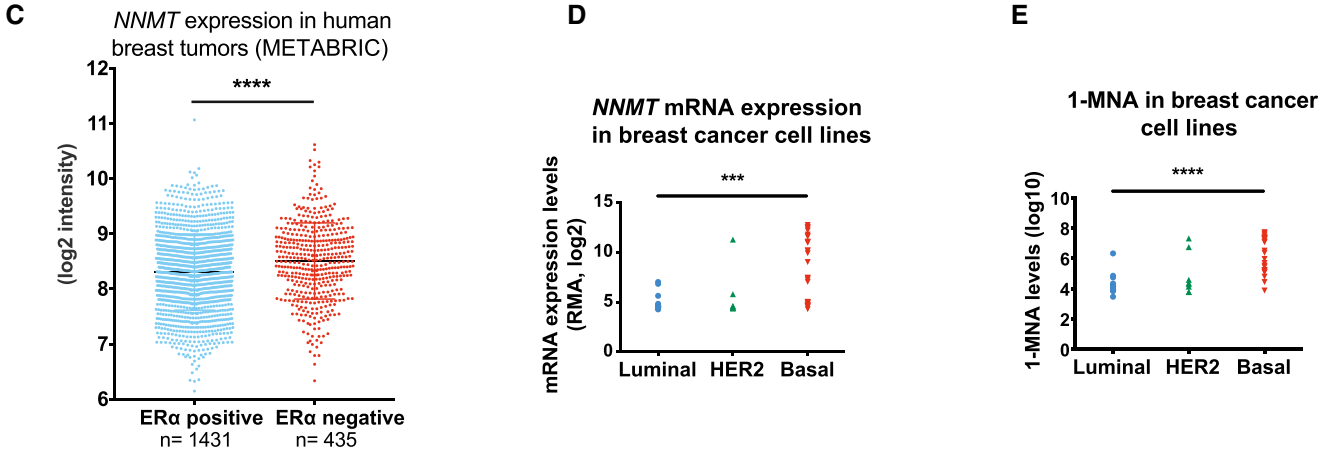

Figure EV1.

Figure EV1. NNMT predicts poor recurrence-free survival and is highly expressed in ERα negative breast cancer.

A Recurrence-free survival plots generated using the Kaplan–Meier Plotter (Győrffy *et al*, 2010) based on signal intensity of the NNMT probe (202237_at) in Affymetrix microarray gene expression data from breast cancer patients of The Cancer Genome Atlas. The cut-off was automatically set to split patients into two groups, high and low. NNMT expression is a strong indicator of poor recurrence-free survival in the basal subset (median survival in months is 37 and 17 in low and high groups, respectively), in the HER2-positive subset (median survival in months is 25.76 and 17 in the low and high groups, respectively), in the luminal A subset (median survival in months is 91.36 and 57.3 in the low and high groups, respectively), and in the luminal B subset (median survival in months is 50.07 and 37.0 in the low and high groups, respectively). The hazard ratio (95% confidence intervals) and log-rank *P* values for each graph are indicated.

B Recurrence-free survival plots generated using the Kaplan–Meier Plotter (Győrffy *et al*, 2010) based on signal intensity of the UGT8 (208358_s_at), COQ2 (213379_at), UGCG (204881_s_at), probes in Affymetrix microarray gene expression data from breast cancer patients of The Cancer Genome Atlas, restricted to the basal subgroup according to the PAM50 classification ($n = 953$). The cut-off was automatically set to split patients into two groups, high and low. The hazard ratio (95% confidence intervals) and log-rank *P* values for each graph are indicated.

C Dot plot showing NNMT expression in ERα-positive vs ERα-negative breast cancer cases in the METABRIC (Curtis *et al*, 2012; Pereira *et al*, 2016) cohort. ****$P < 0.0001$; Student *t*-test. $n = 1866$ patients. Data are means ± SD.

D Dot plot depicting NNMT mRNA expression in breast cancer cell lines from the Cancer Cell Line Encyclopedia (CCLE) atlas (Ghandi *et al*, 2019), ***$P < 0.001$; Student *t*-test.

E Dot plots depicting 1-MNA abundance in breast cancer cell lines from the Cancer Cell Line Encyclopedia (CCLE) atlas (Ghandi *et al*, 2019), ****$P < 0.0001$; Student *t*-test.

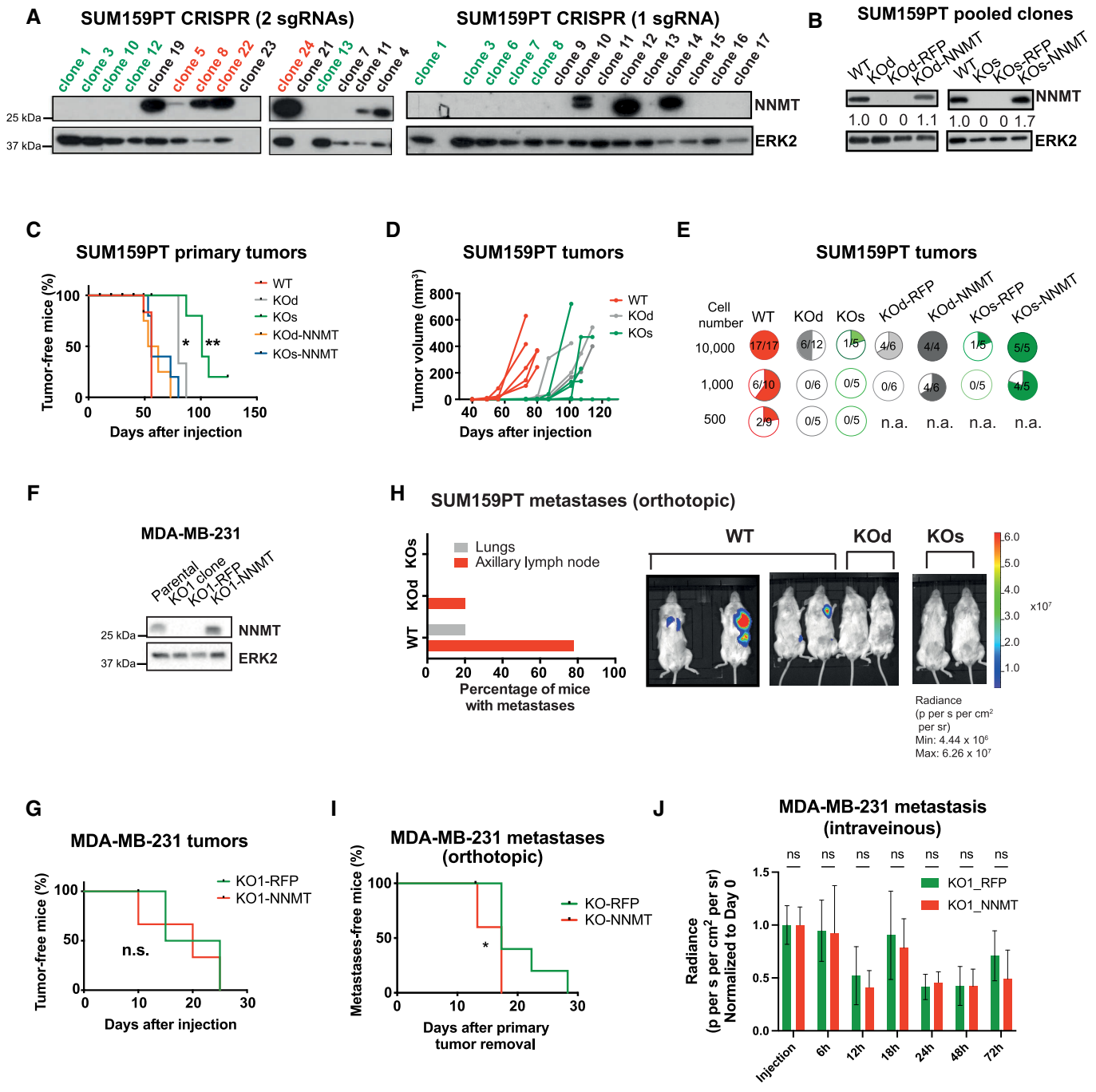
A
SUM159PT CRISPR (2 sgRNAs)
clone 1
clone 3
clone 10
clone 12
clone 19
clone 5
clone 8
clone 22
clone 23
clone 24
clone 21
clone 13
clone 7
clone 11
clone 4
SUM159PT CRISPR (1 sgRNA)
clone 1
clone 3
clone 6
clone 7
clone 8
clone 9
clone 10
clone 11
clone 12
clone 13
clone 14
clone 15
clone 16
clone 17
25 kDa
37 kDa
NNMT
ERK2
B
SUM159PT pooled clones
WT
KOd
KOd-RFP
KOd-NNMT
WT
KOs
KOs-RFP
KOs-NNMT
NNMT
1.0 0 0 1.1
1.0 0 0 1.7
ERK2
C
SUM159PT primary tumors
Tumor-free mice (%)
WT
KOd
KOs
KOd-NNMT
KOs-NNMT
Days after injection
D
SUM159PT tumors
Tumor volume (mm3)
WT
KOd
KOs
Days after injection
E
SUM159PT tumors
Cell number
WT
KOd
KOs
KOd-RFP
KOd-NNMT
KOs-RFP
KOs-NNMT
10,000
1,000
500
17/17
6/12
1/5
4/6
4/4
1/5
5/5
6/10
0/6
0/5
0/6
4/6
0/5
4/5
2/9
0/5
0/5
n.a.
n.a.
n.a.
n.a.
F
MDA-MB-231
Parental
KO1 clone
KO1-RFP
KO1-NNMT
25 kDa
37 kDa
NNMT
ERK2
H
SUM159PT metastases (orthotopic)
KOs
KOd
WT
Lungs
Axillary lymph node
Percentage of mice with metastases
WT
KOd
KOs
x10^7
Radiance (p per s per cm2 per sr)
Min: 4.44 x 10^6
Max: 6.26 x 10^7
G
MDA-MB-231 tumors
Tumor-free mice (%)
KO1-RFP
KO1-NNMT
n.s.
Days after injection
I
MDA-MB-231 metastases (orthotopic)
Metastases-free mice (%)
KO-RFP
KO-NNMT
Days after primary tumor removal
J
MDA-MB-231 metastasis (intraveinous)
Radiance (p per s per cm2 per sr) Normalized to Day 0
KO1_RFP
KO1_NNMT
Injection
6h
12h
18h
24h
48h
72h

Figure EV2.

Figure EV2. NNMT depletion reduces metastases formation in basal breast cancer.

A Immunoblots showing levels of NNMT and ERK2 (loading control) in single-cell derived clones of SUM159PT after NNMT KO using two independent CRISPR-Cas9 strategies (left: KOd, right: KOs). For each group, single-cell clones were pooled in equal proportions to minimize undesired off-target and clonal effects (in red for WT and green for KOd and KOs).

B Immunoblots showing NNMT and ERK2 (loading control) levels in SUM159PT KOd, KOs, and WT pooled clones and the respective rescue cell lines.

C Kaplan–Meier plot depicting tumor onset in mice injected orthotopically with SUM159PT WT (median 56 days; $n = 5$), KO (KOd: median 80 days, $n = 5$; KOs: median 101 days, $n = 5$) or KO-NNMT cells (KOd-NNMT: median 58 days, $n = 4$; KOs-NNMT: median 56 days, $n = 5$). $^{*}P < 0.05$, $^{**}P < 0.01$; log-rank test.

D Graph representing the kinetics of SUM159PT WT ($n = 5$), KOd ($n = 3$), and KOs ($n = 5$) tumor growth upon orthotopic injection of 100,000 cells into NSG mice. The median onset (tumor volume approximately 5 mm^3) is 45, 77 and 85 days for WT, KOd, and KOs tumors, respectively.

E Quantification of tumor incidence (pie charts) in the SUM159PT model upon orthotopic injection into mice of WT, NNMT KO or NNMT rescue cells.

F Immunoblots showing NNMT and ERK2 (loading control) levels in MDA-MB-231 parental cells and in a single KO clone (KO1) and the respective rescue cell lines.

G Kaplan–Meier plot depicting tumor onset in mice injected orthotopically with MDA-MB-231 KO1-RFP (median 20 days; $n = 5$) or KO1-NNMT (median 20 days; $n = 5$). n.s., not significant; log-rank test.

H Bar plot depicting the proportion of organ-specific metastases in mice injected with SUM159PT WT ($n = 9$) or NNMT KO (KOd, $n = 5$ and KOs, $n = 5$) cells. Representative bioluminescence images are shown.

I Kaplan–Meier plot depicting metastasis onset after tumor removal in mice injected with MDA-MB-231 KO1-RFP ($n = 10$) or MDA-MB-231 KO1-NNMT ($n = 4$). $^{*}P < 0.05$; log-rank test. All data are means ± SD.

J Bar graph quantification of luciferase signal from the lungs of NSG mice injected with MDA-MB-231 KO1-RFP or KO1-NNMT cells into the tail vein of mice, right after injection and at 6, 12, 18, 24, 48 and 72 h post-injection. $n = 5$ animals per group. n.s. not significant; the Mann–Whitney *U*-test. All data are means ± SD.

Figure EV3. NNMT depletion promotes loss of basal identity and represses expression of collagens and their processing machinery.

A Heat map depicting the 301 concomitantly downregulated genes in SUM159PT KOd and KOs versus WT cells. $n = 3$ experimental replicates per group. Cut-off: FDR < 0.05, log2 fold change > 0.85.

B, C Pathway enrichment analyses (B: Metascape, C: Reactome) analysis of the 301 commonly downregulated genes depicted in panel (A).

D Ingenuity Pathway Analysis (Upstream Regulators) of the 301 commonly downregulated genes depicted in panel (A).

E Left panel: Representative phase contrast and immunofluorescence images of SUM159PT WT, KOd and KOs cells demonstrating loss of mesenchymal morphology and acquisition of epithelial-like features in NNMT KO cells. Right panel: immunofluorescence quantification ($n = 3$ experimental replicates) showing decreased protein expression of the mesenchymal fibronectin and vimentin markers and the luminal cytokeratins 8/18 in SUM159PT KOd and KOs cell compared to WT cells. $^{*}P < 0.5$, $^{**}P < 0.01$, $^{****}P < 0.0001$; Student *t*-test. Scale bars: 50 μm. Data are means ± SD.

F Left panel: Representative images of NNMT immunostaining in normal breast ducts from 35 breast cancer patients showing preferential expression in the basal cell compartment (arrowhead). Right panel: pie chart quantification of the percentage of NNMT-positive cells within the basal and luminal compartments. Scale bar: 100 μm.

G Bar graph representing average mRNA expression of collagens and collagen processing genes in the MDA-MB-231 cell model upon NNMT KO. $n = 2$–3 experimental replicates with 2–3 technical replicates each. $^{*}P < 0.05$, n.s., not significant; Two-Way ANOVA. All data are means ± SD.

H Venn diagram depicting overlap between the 301 genes commonly downregulated upon NNMT ablation in the SUM159PT KO versus WT comparison and a list of the 10 most described EMT-inducing transcription factors, EMT-TF (*SNAI1*, *SNAI2 TWIST1*, *TWIST2*, *ZEB1*, *ZEB2*, *SOX4*, *SOX9*, *FOXC1*, *FOXC2*).

I Venn diagram depicting overlap between the 301 genes commonly downregulated upon NNMT ablation in the SUM159PT KO versus WT comparison and a list of known collagen binding receptors (*ITGB1*, *ITGA2 ITGA10*, *ITGA11*, *DDR1*, *DDR2*, *GP6*, *LAIR1*, *GPR56*).

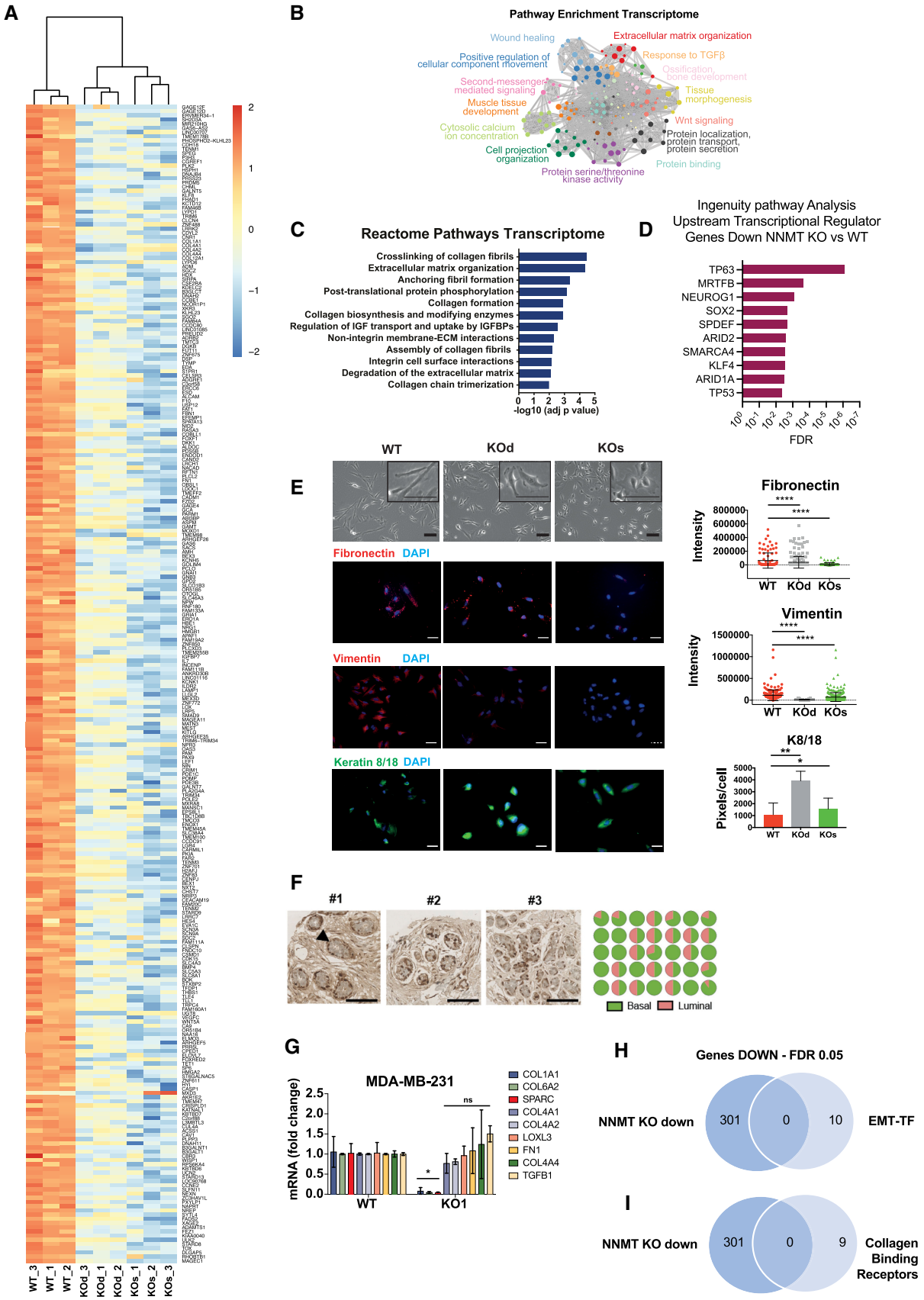
A
WT_3
WT_1
WT_2
KOd_3
KOd_1
KOd_2
KOs_1
KOs_2
KOs_3
B
Pathway Enrichment Transcriptome
Wound healing
Extracellular matrix organization
Positive regulation of cellular component movement
Response to TGFβ
Ossification, bone development
Second-messenger mediated signaling
Tissue morphogenesis
Muscle tissue development
Wnt signaling
Cytosolic calcium ion concentration
Protein localization, protein transport, protein secretion
Cell projection organization
Protein binding
Protein serine/threonine kinase activity
C
Reactome Pathways Transcriptome
Crosslinking of collagen fibrils
Extracellular matrix organization
Anchoring fibril formation
Post-translational protein phosphorylation
Collagen formation
Collagen biosynthesis and modifying enzymes
Regulation of IGF transport and uptake by IGFBPs
Non-integrin membrane-ECM interactions
Assembly of collagen fibrils
Integrin cell surface interactions
Degradation of the extracellular matrix
Collagen chain trimerization
-log10 (adj p value)
D
Ingenuity pathway Analysis
Upstream Transcriptional Regulator
Genes Down NNMT KO vs WT
TP63
MRTFB
NEUROG1
SOX2
SPDEF
ARID2
SMARCA4
KLF4
ARID1A
TP53
FDR
E
WT
KOd
KOs
Fibronectin DAPI
Vimentin DAPI
Keratin 8/18 DAPI
Fibronectin
Intensity
Vimentin
K8/18
Pixels/cell
F
#1
#2
#3
Basal
Luminal
G
MDA-MB-231
mRNA (fold change)
COL1A1
COL6A2
SPARC
COL4A1
COL4A2
LOXL3
FN1
COL4A4
TGFB1
WT
KO1
H
Genes DOWN - FDR 0.05
NNMT KO down
301
0
10
EMT-TF
I
NNMT KO down
301
0
9
Collagen Binding Receptors

Figure EV3.

Figure EV4. PRDM5 enhances collagen gene expression and metastatic colonization.

A Left panel: Venn diagram depicting the intersection of PRDM5 bound genes (Galli *et al*, 2012) with genes commonly downregulated in NNMT KOs and KOd cells. $n = 3$ experimental replicates. Cut-off: FDR < 0.05, Log2 fold change > 0.85. Right panel: Pathway analysis (BioPlanet – 2019) of the 18 genes identified in the upper panel. Dark blue bars highlight ECM and collagen-associated terms.

B Dot plot depicting PRDM5 mRNA expression in SUM159PT WT, KOd, KOs and PRDM5 over-expression lines ($n = 2$ experimental replicates, with two technical replicates). ****$P < 0.0001$, n.d., not detected; One-Way ANOVA. Central band indicates the mean.

C Bar graph representing average collagen gene mRNA expression upon overexpression of PRDM5 from its endogenous promoter using CRISPR-Activating technology in SUM159PT parental cells. $n = 3$ experimental replicates with two technical replicates each. *$P < 0.05$, n.s., not significant; Kruskal–Wallis test. Data are means ± SEM.

D Gene set enrichment analysis (C2 – Curated GSEA, breast cancer-related gene signatures) of the top 500 genes displaying promoter CpG hypermethylation upon NNMT KO (FDR > 0.05).

E Bar graphs depicting 5-mC abundance at promoters of indicated genes shown as fold enrichment of methylated DNA immunoprecipitate (MedIP) over IgG control. $n = 3$ experimental replicates with 2 to 3 technical replicates each. n.s., not significant; Kruskal–Wallis test. All data are means ± SEM.

F Bar graphs representing PRDM5 and COL1A1 mRNA expression in MDA-MB-231 cells expressing sh NT or sh PRDM5. $n = 4$ experimental replicates. *$P < 0.05$, **$P < 0.01$, ***$P < 0.001$, n.s., not significant; Mann–Whitney *U*-test. All data are means ± SEM.

G Left panel: bar graph quantification of lung metastatic positive area in the different conditions. $n = 4$ to 5 lungs per condition. *$P < 0.05$, **$P < 0.01$; One-way ANOVA. All data are means ± SEM. Right panel: representative images of MDA-MB-231 lung metastatic *foci* stained with HE staining, in sh NT and sh PRDM5 experimental conditions. Scale bar: 1 cm.

H Bar graph showing quantification of Cell Titer GLO assay comparing MDA-MB-231 cells expressing sh NT or sh PRDM5. $n = 6$ experimental replicates. n.s., not significant; One-way ANOVA. All data are means ± SD.

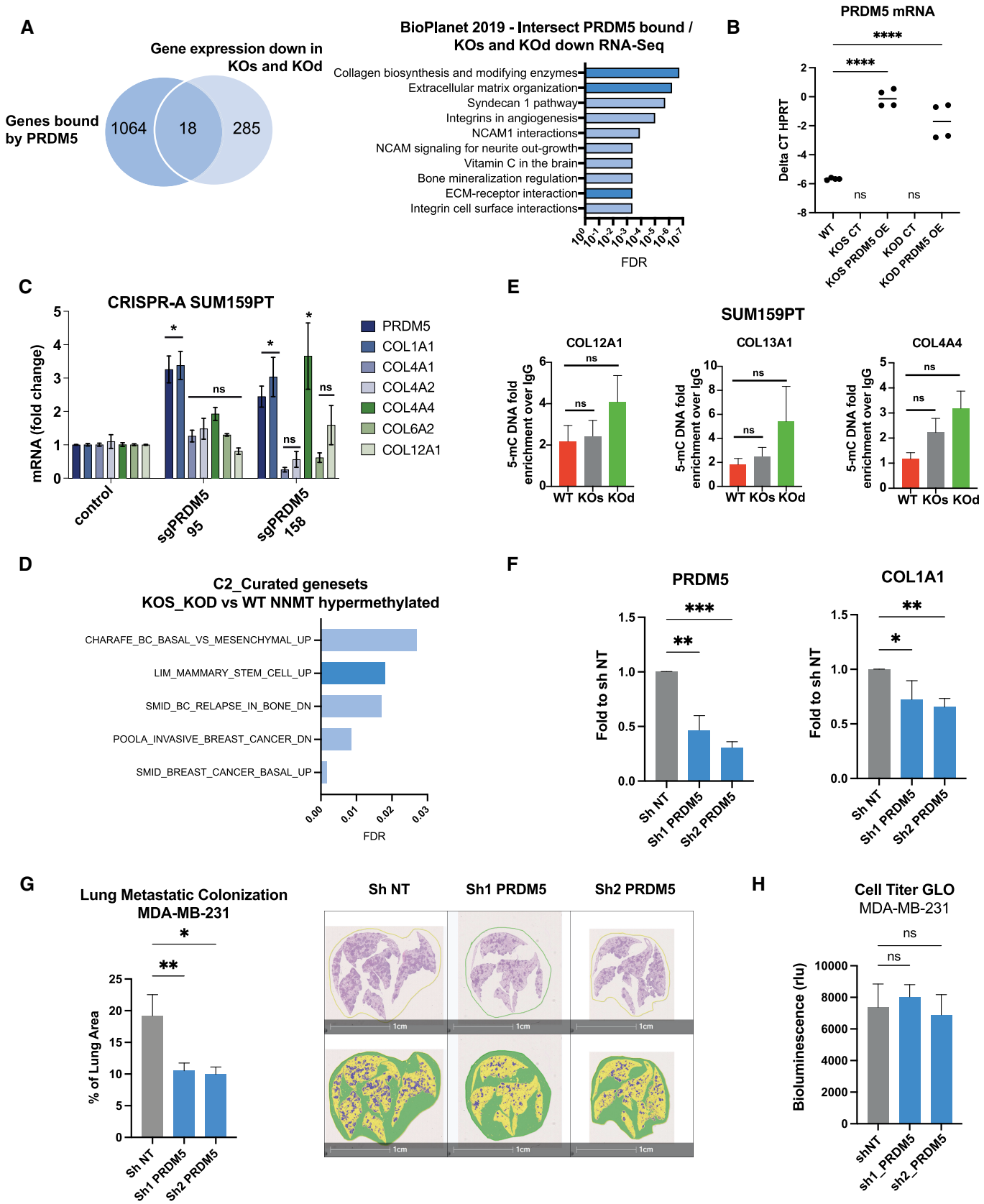
A
Gene expression down in KOs and KOd
Genes bound by PRDM5
1064
18
285
BioPlanet 2019 - Intersect PRDM5 bound / KOs and KOd down RNA-Seq
Collagen biosynthesis and modifying enzymes
Extracellular matrix organization
Syndecan 1 pathway
Integrins in angiogenesis
NCAM1 interactions
NCAM signaling for neurite out-growth
Vitamin C in the brain
Bone mineralization regulation
ECM-receptor interaction
Integrin cell surface interactions
FDR
B
PRDM5 mRNA
Delta CT HPRT
WT
KOS CT
KOS PRDM5 OE
KOD CT
KOD PRDM5 OE
C
CRISPR-A SUM159PT
mRNA (fold change)
PRDM5
COL1A1
COL4A1
COL4A2
COL4A4
COL6A2
COL12A1
control
sgPRDM5 95
sgPRDM5 158
E
SUM159PT
COL12A1
COL13A1
COL4A4
5-mC DNA fold enrichment over IgG
WT KOs KOd
D
C2_Curated genesets
KOS_KOD vs WT NNMT hypermethylated
CHARAFE_BC_BASAL_VS_MESENCHYMAL_UP
LIM_MAMMARY_STEM_CELL_UP
SMID_BC_RELAPSE_IN_BONE_DN
POOLA_INVASIVE_BREAST_CANCER_DN
SMID_BREAST_CANCER_BASAL_UP
FDR
F
PRDM5
COL1A1
Fold to sh NT
Sh NT
Sh1 PRDM5
Sh2 PRDM5
G
Lung Metastatic Colonization
MDA-MB-231
% of Lung Area
Sh NT
Sh1 PRDM5
Sh2 PRDM5
1cm
H
Cell Titer GLO
MDA-MB-231
Bioluminescence (rlu)
shNT
sh1_PRDM5
sh2_PRDM5

Figure EV4.

Figure EV5. Immuno-histochemical staining of COL1A1 and PRDM5, digital analysis, and clinical association with relapse-free-survival.

A Bar graph showing COL1A1 mRNA expression in MDA-MB-231 KO1_RFP, KO1_NNMT and KO1_COL1A1 (COL1A1 over expression) cells. $n = 3$ experimental replicates. ***$P < 0.001$; One-way ANOVA. All data are means ± SD.

B Bar graph showing quantification of Cell Titer GLO assay comparing MDA-MB-231 cells expressing sh NT or sh COL1A1. $n = 6$ experimental replicates. n.s., not significant; Student *t*-test. Data are means ± SD.

C, D Representative COL1A1 and PRDM5 staining of breast cancer tissues cores of the tissue-microarrays (TMAs, left). Classes used for training a deep neural network algorithm: The red area corresponds to the tumor; stroma has been sub-classified into desmoplastic (green) and inflamed (blue) (middle). Heatmap showing differential expression of the respective markers (right). COL1A1; Scale bar, 200 μm. PRDM5; Scale bar, 100 μm.

E Dot plot showing COL1A1 expression level (H-Score) across the different sample types: normal tissue ($n = 76$) or primary tumor (PT, $n = 757$) ****$P < 0.0001$, Student *t*-test.

F Dot plot showing COL1A1 expression level (H-Score) across the different areas of the tissue section: tumor epithelium versus stroma ($n = 857$). ****$P < 0.0001$; Student *t*-test.

G Bar Graph showing COL1A1 expression level (H-Score) according to the NNMT status within all tumor samples. NNMT (−) negative, $n = 193$; NNMT (+) positive, $n = 170$. n.s., non-significant; Student *t*-test. Boxes define the upper and lower quartiles; central band indicates the median; whiskers define max to min values.

H Dot plot showing correlation of PRDM5 (*x*-axis) and COL1A1 (*y*-axis) H-scores inferred from HR–negative tumor patient samples from the TMA ($n = 64$), *$P < 0.05$ correlation *P*-value. Pearson index is indicated.

I Kaplan–Meier plot depicting survival of breast cancer patients stratified according to COL1A1 protein levels (H-Score) specifically in the tumor epithelium area ($n = 857$; median cut-off). Estimated 10-year overall survival rates are 37 (medium/high COL1A1 group) and 43 months (low/negative COL1A1 group), respectively. **$P < 0.01$; log-rank test.

J Recurrence-free survival plots generated using the Kaplan–Meier Plotter based on signal intensity of COL1A1 (202311_s_at) probe in Affymetrix microarray gene expression data from breast cancer patients of The Cancer Genome Atlas (Györffy *et al*, 2010), in the luminal A ($n = 1809$), HER2-enriched ($n = 695$) and basal ($n = 953$) subgroups according to the PAM50 classification. The cut-off was automatically set to split patients into two groups, high and low. The hazard ratio (95% confidence intervals) and log-rank *P*-values for each graph are indicated.

K Kaplan–Meier survival analysis of breast cancer patients stratified according to PRDM5 protein levels (H-Score) specifically in the tumor epithelium area ($n = 857$; median cut-off). Estimated 10-year overall survival rates. n.s., non-significant; log-rank test.

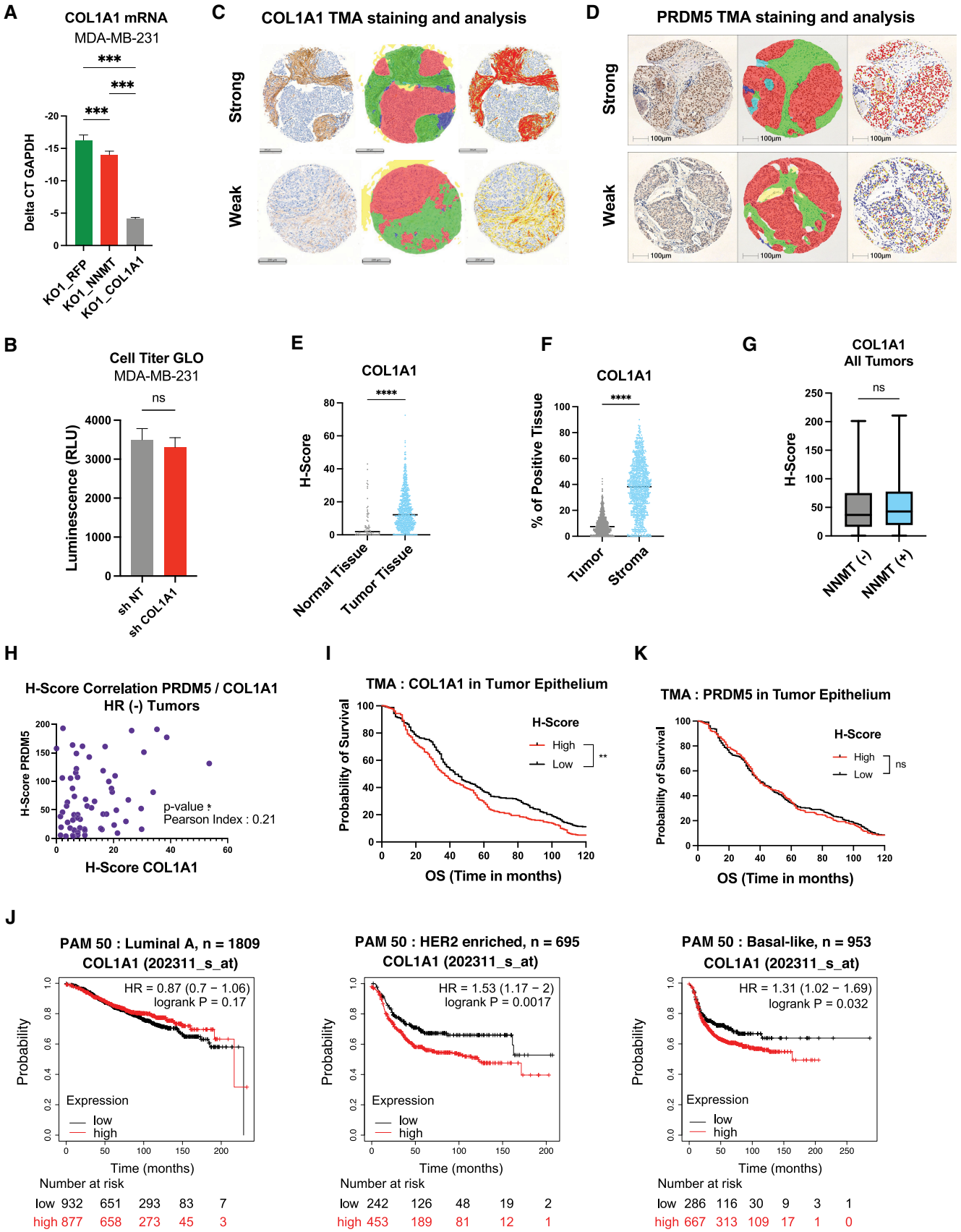

Figure EV5.